Characterization of the L_λ Phase in Trehalose-Stabilized Dry Membranes by Solid-State NMR and X-ray Diffraction†

C. W. B. Lee,‡,§ S. K. Das Gupta,§ J. Mattai,‖ G. G. Shipley,‖ O. H. Abdel-Mageed,⊥ A. Makriyannis,⊥ and R. G. Griffin*,§

Department of Chemistry and Francis Bitter National Magnet Laboratory, Massachusetts Institute of Technology, Cambridge, Massachusetts 02139, Department of Biophysics, Boston University School of Medicine, Boston, Massachusetts 02118, and Department of Medicinal Chemistry, University of Connecticut, Storrs, Connecticut 06268

Received December 5, 1988; Revised Manuscript Received February 7, 1989

ABSTRACT: Solid-state nuclear magnetic resonance (NMR) spectroscopy and X-ray powder diffraction were used to investigate the mechanism of trehalose (TRE) stabilization of lipid bilayers. Calorimetric investigation of dry TRE-stabilized bilayers reveals a first-order phase transition ($L_\kappa \rightarrow L_\lambda$) at temperatures similar to the $L_{\beta'} \rightarrow (P_{\beta'}) \rightarrow L_\alpha$ transition of hydrated lipid bilayers. X-ray diffraction studies show that dry mixtures of TRE and 1,2-dipalmitoyl-*sn*-phosphatidylcholine (DPPC) have a lamellar structure with excess crystalline TRE being present. The L_κ phase shows typical gel-phase X-ray diffraction patterns. In contrast, the L_λ-phase diffraction patterns indicate disordered hydrocarbon chains. ^2H NMR of specifically ^2H chain-labeled DPPC confirmed that the acyl chains are disordered in the L_λ phase over their entire lengths. ^2H spectra of the choline headgroup show hindered molecular motions as compared to dry DPPC alone, and ^{13}C spectra of the *sn*-2-carbonyl show rigid lattice powder patterns indicating very little motion at the headgroup and interfacial regions. Thus, the sugar interacts extensively with the hydrophilic regions of the lipid, from the choline and the phosphate moieties in the headgroup to the glycerol and carbonyls in the interfacial region. We postulate that the sugar and the lipid form an extensive hydrogen-bonded network with the sugar acting as a spacer to expand the distance between lipids in the bilayer. The fluidity of the hydrophobic region in the L_λ phase together with the bilayer stabilization at the headgroup contributes to membrane viability in anhydrobiotic organisms.

Until recently, very little was known about the role of sugars and an organism's ability to survive stressful environmental conditions. Research into anhydrobiosis, the ability to survive dehydration and rehydration, has revealed that sugars can play an important role in maintaining cell viability under dry conditions (Crowe & Clegg, 1973, 1979; Leopold, 1986). In a variety of anhydrobiotic organisms—certain fungi, nematodes, brine shrimp, and yeast—trehalose (TRE),[1] a nonreducing disaccharide of glucose whose structure is shown in Figure 1, can be found in concentrations of up to 20% of the dry weight of the dehydrated organism (Clegg, 1965; Madin et al., 1979) where it apparently stabilizes the bilayer structure of the dry membrane. It has been postulated that the disaccharide exerts this effect by replacing the water of hydration surrounding the lipids in the bilayer (Clegg et al., 1982; Crowe & Crowe, 1984).

The mechanism by which sugar–lipid interactions stabilize dry membranes is not well understood. The effects that TRE exert on biological membranes have been studied by assaying the biological activity in rehydrated membranes from organisms which do not normally survive dehydration and rehydration. For instance, microsomes of lobster muscle lose all activity when dried and rehydrated, while those dehydrated in the presence of TRE maintained almost full biological activity (Crowe, L. M., et al., 1984; Crowe et al., 1986). In addition, electron microscopy revealed that dehydrated and rehydrated microsomes sustained extensive damage, whereas those stabilized with TRE showed no gross morphological changes (Crowe et al., 1983). Although insightful on a macroscopic level, these studies do not reveal the microscopic, molecular mechanism of TRE stabilization of dry membranes.

The heterogeneity of biological membranes can complicate studies of the essential features of TRE–lipid interactions, and, therefore, single-component model membrane systems provide an opportunity to obtain more insight into sugar stabilization. Sugars are known to expand phospholipid monolayer films, with TRE being one of the most effective (Johnston et al., 1984). However, surface-active impurities render some of these observations inconclusive (Arnett et al., 1986). In addition, IR spectra show shifts associated with the phosphate group of the lipid (Crowe, J. H., et al., 1984) suggesting that the disaccharide may interact with the PO_4 group. DSC scans indicate that TRE is able to depress the first-order phase transition in dry phospholipids to a temperature close to that of hydrated bilayers (Crowe, J. H. et al., 1984), leading to a transition which we have labeled $L_\kappa \rightarrow L_\lambda$ (Lee et al., 1986). In addition, a model for TRE-stabilized bilayers has been derived by utilizing energy minimization routines to calculate the conformation of TRE in a crystal lattice of DMPC (Chandrasekhar & Gaber, 1988). To date, there has been no conclusive evidence on the molecular level to confirm or disprove this model.

Using solid-state NMR techniques, we have elucidated some of the molecular details of TRE-stabilized bilayers containing

† This research was supported by the National Institutes of Health (GM-25505, RR-00995, HL-26335, and HL-07429), the National Institute on Drug Abuse (DA-3801), and Glaxo Laboratories (Grant 642). C.W.B.L. received fellowship support from the Natural Sciences and Engineering Research Council of Canada.

‡ Department of Chemistry, MIT.
§ Francis Bitter National Magnet Laboratory, MIT.
‖ Boston University School of Medicine.
⊥ University of Connecticut.

[1] Abbreviations: DMPC, 1,2-dimyristoyl-*sn*-phosphatidylcholine; DPPC, 1,2-dipalmitoyl-*sn*-phosphatidylcholine; DPPE, 1,2-dipalmitoyl-*sn*-phosphatidylethanolamine; DSC, differential scanning calorimetry; IR, infrared spectroscopy; NMR, nuclear magnetic resonance; TRE, trehalose; T_m, lipid chain melting temperature.

0006-2960/89/0428-5000$01.50/0

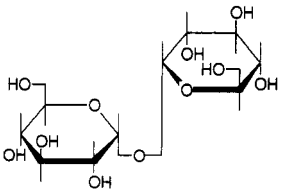

FIGURE 1: Molecular structure of trehalose.

the model phospholipid DPPC (Lee et al., 1986). ^{31}P and ^{2}H NMR spectra of dry TRE/DPPC mixtures exhibit features that are distinctly different from either the hydrated or the dry lipid bilayer. Apparently, the sugar interacts with the headgroup, possibly through hydrogen bonding, and hinders axial diffusion of the lipid. The sugar–headgroup interaction also expands the intermolecular spacing of the lipids, so that the hydrocarbon chains are free to assume gauche conformations above T_m.

In this paper, we present solid-state NMR and X-ray powder diffraction results that provide additional insight into the dynamic structure of TRE-stabilized phospholipid bilayers. X-ray diffraction data indicate that TRE-stabilized lipids form lamellar phases. Furthermore, we find that a matrix of sugar surrounds the bilayer, so that at the sample concentration of 2:1 TRE/DPPC used in these studies, there is an excess amount of TRE present, and we are thus observing the full effects of the sugar on the bilayer structure. ^{2}H quadrupole echo spectra of TRE/DPPC mixtures with ^{2}H labeled at the choline headgroup show that TRE restricts headgroup motion as compared to either dry or hydrated DPPC. ^{13}C NMR spectra of TRE/DPPC mixtures, with ^{13}C labeled at the *sn*-2 carbonyl, indicate that the sugar totally inhibits motion of the lipid molecule in the interfacial region. From these spectra, it is clear that axial diffusion of the lipids is absent in the TRE/DPPC L_κ bilayers, in contrast to hydrated $L_{\beta'}$ bilayers. Upon passing through the $L_\kappa \rightarrow L_\lambda$ phase transition, the ^{31}P spectra (Lee et al., 1986) and ^{13}C spectra of the *sn*-2-carbonyl remain at their full static breadth. In contrast, the ^{2}H spectra of TRE/DPPC mixtures with chain-labeled DPPC narrowed by a factor of $\sim$4. The line shapes are also very distinctive and can be simulated by using a hopping model involving four sites of tetrahedral geometry reflecting trans-gauche isomerization of the hydrocarbon chain.

On the basis of the structural and dynamic information as revealed by X-ray diffraction and NMR, we have identified a new set of phases for dehydrated bilayers which we denote as L_κ and L_λ, corresponding to the phases below and above the main transition of the TRE–lipid mixture. One basic feature of the L_κ and L_λ phases is the immobilization of the headgroup portion of the lipid molecule. Of the two, the L_λ phase is the most interesting as it contains features that mimic the L_α phase of hydrated lipids. Thus, these studies reveal, in part, the mechanism by which TRE preserves membrane integrity in the dry state and aids survival of an organism upon dehydration.

Experimental Procedures

Materials. TRE was obtained from Pfanstiehl Laboratories Inc. (Waukegan, IL). 2[4,4-$^{2}H_2$]DPPC and 2[12,12-$^{2}H_2$]-DPPC were synthesized by Avanti Polar Lipids (Birmingham, AL) using [4,4-$^{2}H_2$]palmitic acid and [12,12-$^{2}H_2$]palmitic acid prepared in this laboratory according to previously published methods (Das Gupta et al., 1982). 2[1-^{13}C]DPPC was prepared by acylation of 1-palmitoyl-*sn*-phosphatidylcholine with [1-^{13}C]palmitic acid anhydride using *N*,*N*-dimethyl-4-aminopyridine as a catalyst (Gupta et al., 1977).

$N(C^{2}H_3)_3$-DPPC was synthesized from DPPE obtained from Sigma Chemical Co. (St. Louis, MO) and deuterated methyl iodide from Aldrich Chemical Co. (Milwaukee, WI) using the following procedure which is a modification of a previously published method (Patel et al., 1979). The changes were necessitated because of the insolubility of DPPE in benzene. Anhydrous potassium carbonate (284 mg, 2.06 mmol) and 18-crown-6 (1488 mg, 5.63 mmol) were dissolved in dry benzene (5 mL). The mixture was stirred for 20 min at 25 °C. Then a slurry of DPPE (1000 mg, 1.45 mmol) in dry benzene (5 mL) was added, followed by the deuterated methyl iodide (830 mg, 5.73 mmol). The reaction tube was sealed under nitrogen and gradually heated in an oil bath to 40 °C. After 2 h, an additional aliquot of deuterated methyl iodide (830 mg, 5.73 mmol) was added and the reaction mixture stirred for an additional 12 h. The reaction mixture was cooled to 25 °C, distilled water (25 mL) was added, and then the product was extracted with benzene (3 × 25 mL). The solvent was evaporated and the crude residue was purified using column chromatography (silica gel 60, Aldrich Chemical Co.). The column was eluted first with chloroform and then with a chloroform/methanol mixture, gradually increasing the methanol content from 5 to 60%. The last eluent was chloroform/methanol/water (60:30:4 v/v) to give the product as a white microcrystalline solid (175 mg, 67.4%).

NMR Spectroscopy. Dry DPPC and TRE/DPPC NMR samples (50–100 mg) were prepared by lyophilization with 2:1 (v/v) methanol/benzene as solvent. The lyophilized material was placed in 7-mm glass tubes, pumped at 10^{-6} torr for 1–2 days to remove all residual solvent, and sealed under vacuum. All samples were checked by DSC using a Perkin-Elmer DSC-2 (Perkin-Elmer Corp., Norwalk, CT) at each step of the sample preparation procedure to ensure sample integrity and that no phase separation occurred. All TRE/DPPC samples exhibited a metastable transition at approximately 48 °C (Lee et al., 1986). Hydrated DPPC samples were prepared by dispersing the lipid in ^{2}H-depleted H_2O and sealing under vacuum. ^{13}C and ^{2}H NMR spectra were obtained on a home-built solid-state NMR spectrometer operating at 9.35 T (61.05 MHz for ^{2}H, 100.00 MHz for ^{13}C, and 397.7 MHz for ^{1}H). ^{13}C spectra were recorded using a Hahn echo or cross-polarization with a 180° refocusing pulse to minimize base-line distortion (Pines et al., 1973; Griffin, 1981). Typical 90° pulse widths were 6.0 μs for ^{13}C and 3.5 μs for ^{1}H. ^{2}H spectra were recorded using a quadrupole echo with a pulse spacing of 40 μs (Davis et al., 1976) and a typical 90° pulse width of 1.8–2.5 μs. Because of the short pulse widths, corrections for the power roll-off (Bloom et al., 1980) were small. Temperature control to 0.5 °C was achieved with a gas flow system described elsewhere (Wittebort et al., 1981). ^{13}C NMR spectra are referenced to external tetramethylsilane (TMS).

X-ray Diffraction. X-ray diffraction patterns were recorded with photographic films using nickel-filtered Cu Kα X radiation (λ = 1.5418 Å) from an Elliot GX-6 rotating anode generator (Elliott Automation, Borehamwood, U.K.). The X-rays were collimated by toroidal optics into a point source. Samples were mounted in a variable-temperature sample holder with a temperature stability of ±1 °C.

Results

Phase Transitions as a Measure of Dryness. A few remarks about the phase transition temperatures of the TRE/DPPC samples are necessary. It is very difficult to produce anhydrous phospholipid samples, since lyophilization of phospholipids from organic solvents such as methanol and benzene yields

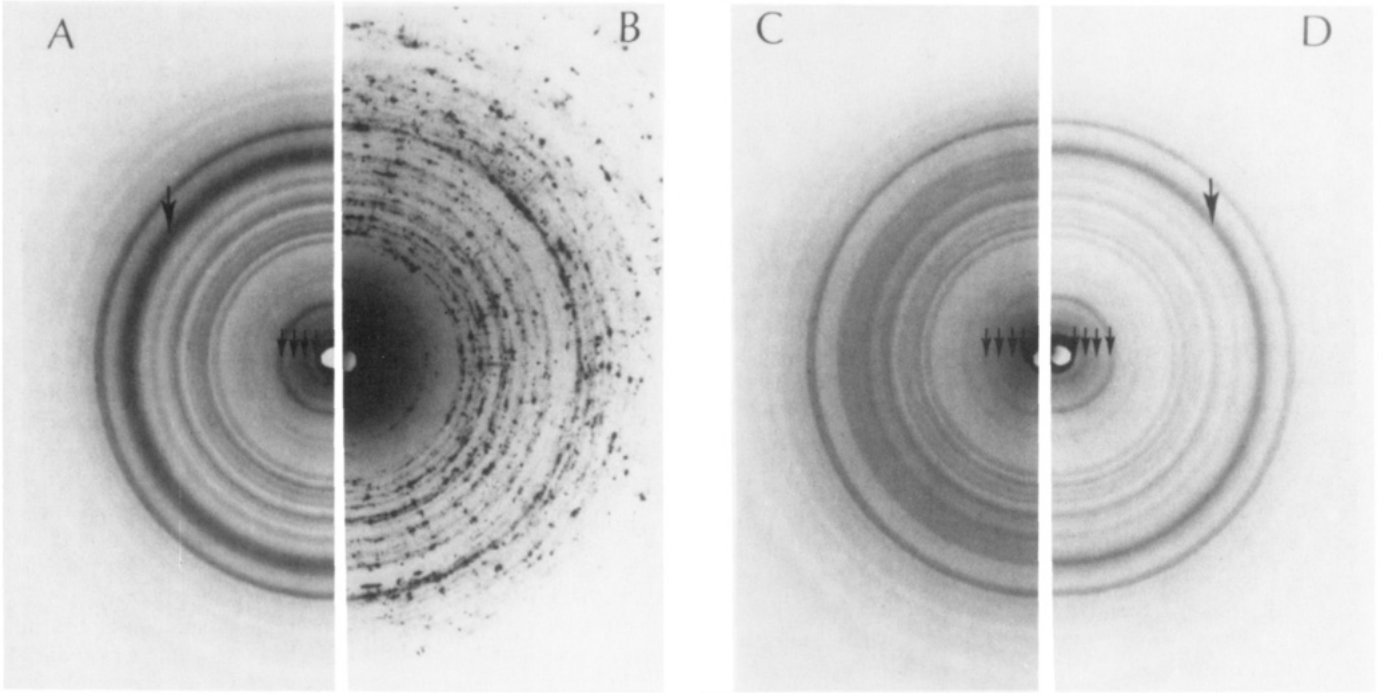

FIGURE 2: X-ray diffraction patterns of a 1.9:1 TRE/DPPC mixture obtained as a function of temperature. (A) 1.9:1 TRE/DPPC at 22 °C before heating. (B) Pure TRE at 22 °C. (C) 1.9:1 TRE/DPPC heated to 56 °C above the $L_\kappa \rightarrow L_\lambda$ transition temperature of 49 °C. (D) 1.9:1 TRE/DPPC recooled to 22 °C.

the dihydrate form (Chapman et al., 1967). If the sample is placed under vacuum and heated above its T_m for an extended period, it is possible to create the monohydrate form. However, for anhydrous samples, more severe conditions are necessary, giving rise to the possibility of sample decomposition. Given our sample preparation procedure, we assume that all "dry" DPPC samples are in the dihydrate form which yields a phase transition temperature of 65 °C (Chapman et al., 1967). There may be variability in the T_m of individual samples with more anhydrous samples (i.e., those containing a mixture of mono- and dihydrate forms) exhibiting slightly higher T_m's.

In TRE/DPPC mixtures, the metastability of the $L_\kappa \rightarrow L_\lambda$ phase transition was used a measure of "dryness". In our experience, lyophilization from methanol/benzene results in a first-order phase transition at ~42 °C with the T_m varying slightly (±2 °C) from sample to sample. This transition is fully reversible and, judging from the NMR spectra, is due to partial hydration of the bilayer. This is not surprising since both the TRE and DPPC used in these samples are obtained in the dihydrate form. Lyophilization from methanol alone is not very efficient in removing bound H_2O, and, hence, a substantial amount of H_2O may remain in the sample, up to a maximum of 6 H_2O/DPPC molecule in a 2:1 TRE/DPPC mixture. Subjecting the samples to a vacuum of 10^{-5}–10^{-6} torr for >1 day drives off all loosely bound H_2O and results in a metastable, elevated T_m of ~48 °C (±2 °C). However, more severe conditions such as heating the sample while it is held under a vacuum in an effort to remove the tightly bound H_2O usually result in phase separation of TRE from the DPPC. This observation suggests that tightly bound H_2O molecules remain in these samples and also contribute to stabilization of the mixtures. As with the dry DPPC samples, there is a certain amount of variability in the T_m due to variation in residual H_2O in each sample. Due to these factors, quality control of sample preparation is of utmost importance, and, hence, all samples used in these studies were frequently monitored by DSC to ensure no phase separation occurred.

X-ray Diffraction Results. X-ray diffraction patterns of a 1.9:1 TRE/DPPC mixture at 22 and 56 °C and recooled to 22 °C are shown in Figure 2. The X-ray diffraction pattern for a sample of pure TRE, lyophilized and vacuum-dried by using the same procedure as for the TRE/DPPC mixtures, is shown as well. The diffraction patterns at all temperatures show a large number of reflections in both the low- and wide-angle regions. At 22 °C before heating (Figure 2A), the low-angle diffraction spacings index in the ratio 1:1/2:1/3:1/4, ..., indicative of a lamellar phase with a bilayer periodicity, d, of 60.6 Å. This bilayer periodicity corresponds to an intermediate value between dry DPPC (58 Å) and fully hydrated DPPC (64 Å). The wide-angle region shows multiple reflections, from approximately 10 to 2 Å, which are due to the presence of excess TRE in the samples (see Figure 2A,B). Noticeable among these reflections is the very strong, broad reflection at 4.11 Å, characteristic of a bilayer gel phase, L_β. Because of the complexity of the wide-angle diffraction pattern, it is not clear if the hydrocarbon chains of the gel phase are tilted (Tardieu et al., 1973; Janiak et al., 1979). Thus, we identify this low-temperature form as a gel phase of DPPC (L_κ, see below), confirming the tentative previous assignment (Lee et al., 1986).

At 56 °C (Figure 2C), above the phase transition temperature as determined by DSC, both the intensity and periodicity of the low-angle reflections change. The reflections still index in the ratio 1:1/2:1/3:1/4, ..., characteristic of a lamellar geometry, but with a reduced periodicity of 52.7 Å. Note the disappearance of the very strong and broad 4.11-Å wide-angle reflection, indicating the loss of the gel phase. Above the phase transition temperature at 56 °C, a broad and diffuse reflection at ~4.5 Å, characteristic of melted hydrocarbon chains of DPPC, should be present. Comparison with the diffraction pattern of pure TRE (Figure 2B) indeed suggests the presence of diffuse scattering in the 4.5-Å region. This together with the absence of a 4.11-Å reflection and the reduction in bilayer periodicity would suggest the presence of a melted liquid-crystalline phase at 56 °C. A comparison of Figure 2A and Figure 2C shows a number of wide-angle reflections below and above the phase transition temperature; most of these reflections are due to the presence of excess TRE

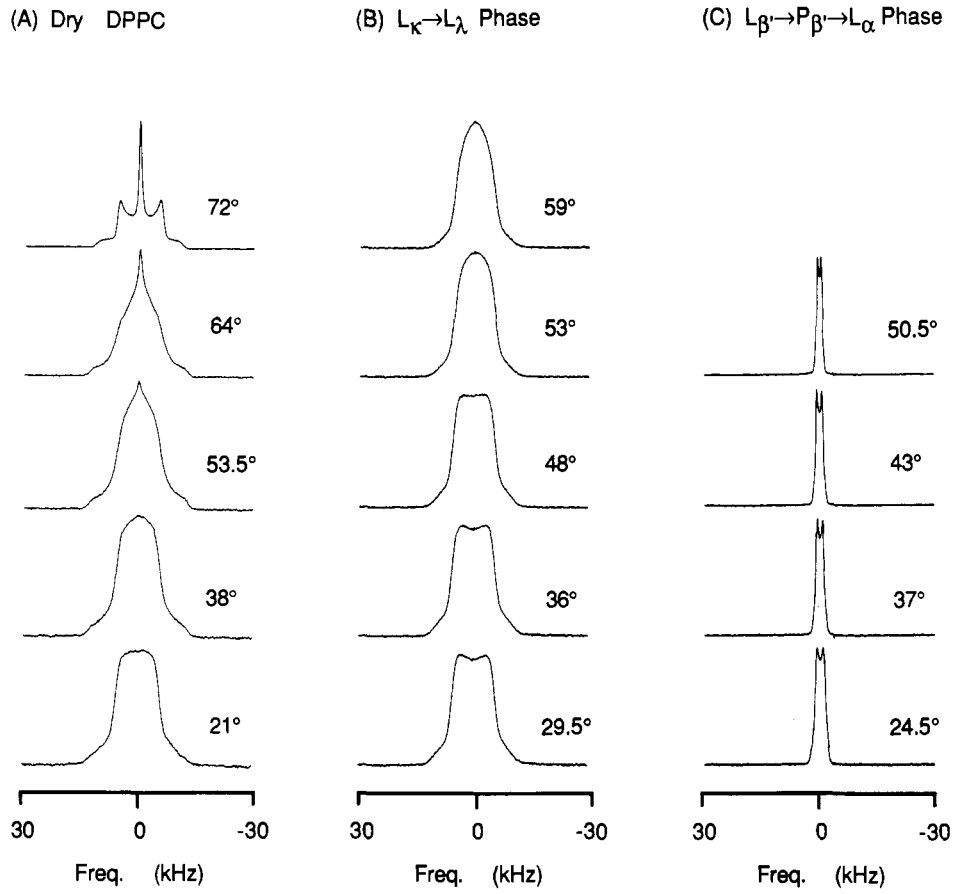

FIGURE 3: Experimental 61.047-MHz ^2H NMR spectra of $N(C^2H_3)_3$-DPPC obtained as a function of temperature. Quadrupole echo with τ = 40 μs. (A) Dry $N(C^2H_3)_3$-DPPC; T_m = 65 °C. (B) 2.14:1 TRE/$N(C^2H_3)_3$-DPPC; $L_\kappa \rightarrow L_\lambda$ transition at 49 °C. (C) Hydrated $N(C^2H_3)_3$-DPPC; $L_{\beta'} \rightarrow P_{\beta'}$ transition at 33 °C, $P_{\beta'} \rightarrow L_\alpha$ transition at 43 °C.

(see Figure 2B). Below the phase transition temperature, the TRE/DPPC mixture therefore exists as a lamellar gel-phase structure in a matrix of excess TRE. Above the transition temperature, the matrix of TRE is maintained, and a melted chain lamellar structure is present. Consistent with the above nomenclature, this phase is designated as L_λ.

On cooling to 22 °C (Figure 2D), the low-angle reflections revert to their original intensity distribution before heating (compare panels A and D of Figure 2) with the bilayer structure now indexing with a slightly reduced periodicity of 58.4 Å. Note the reappearance of the strong and somewhat sharper reflection at 4.12 Å, compared to that observed before heating (see Figure 2A). Again, the characteristic reflections from excess TRE are clearly observed. From differences in the X-ray diffraction patterns, it is clear that the recooled gel phase is similar, but not quite identical in chain packing, to the gel phase before heating. We believe the X-ray results reflect the metastability detected by DSC.

Diffraction patterns (not shown) were also recorded for a 2:1 TRE/DPPC mixture at 22, 56, and 22 °C following cooling. The results were similar to those obtained above for the 1.9:1 TRE/DPPC mixture, but with minor changes in bilayer periodicity. At 22 °C a lamellar gel phase (d = 59.9 Å) and excess TRE are present, while a melted chain bilayer structure with reduced periodicity (d = 56.2 Å) and excess TRE exist at 56 °C. On cooling, the bilayer gel phase is re-formed with a reduced periodicity of 57.8 Å. Although the bilayer periodicity varies from sample to sample, the pattern of behavior is identical.

Molecular Dynamics of the Choline Headgroup. A ^2H NMR temperature dependence study of $N(C^2H_3)_3$-DPPC is shown in Figure 3 where we compare spectra obtained from dry, hydrated, and TRE-stabilized DPPC bilayers. Spectra of dry $N(C^2H_3)_3$-DPPC are shown in Figure 3A, and at 21 °C, the spectrum consists of a flat-topped line shape with a line width of 12.2 kHz and wider shoulders of 24.4 kHz. As the temperature is increased, the line shape grows more rounded in the center and finally evolves into a Pake doublet with a splitting $\Delta\nu_{Q\perp}$ of 10.6 kHz above the phase transition of 65 °C. The spectrum also shows an isotropic peak which comprises ~10% of the integrated intensity of the spectrum. The origin of this spike is unclear, since it is present only as the sample is heated. DSC and TLC on the samples revealed no impurities, so we believe it is due to fast motions in amorphous regions in the sample. Similar spikes have been noted in polycrystalline C^2H_3-labeled trimethylamine (Vega & Luz, 1987) and acetylcholine samples (K. Beshah, private communication).

The value for the Pake doublet splitting is similar to the $\Delta\nu_{Q\perp}$ observed for deuterated trimethylamine (Vega & Luz, 1987) and acetylcholine (K. Beshah, unpublished results). Detailed study of the molecular dynamics of acetylcholine showed that a nine-site motional model incorporating fast-limit internal rotation of the deuterons in the methyl groups coupled with fast-limit reorientation of the methyl groups around the nitrogen atom would give rise to the observed Pake doublet splitting of 13 kHz. In general, fast motions incorporating three-site hops such as the reorientation of methyl groups in alanine give rise to an averaged spectrum with $\Delta\nu_{Q\perp} \simeq$ 38–40 kHz which is a factor of 3 smaller than the rigid lattice splitting of 120 kHz. Three-site reorientation of the methyl groups around the C–N direction introduces an additional factor of 3, thus reducing the splitting to ~13 kHz. In the case of $N(C^2H_3)_3$-DPPC, $\Delta\nu_{Q\perp}$ is slightly smaller, probably

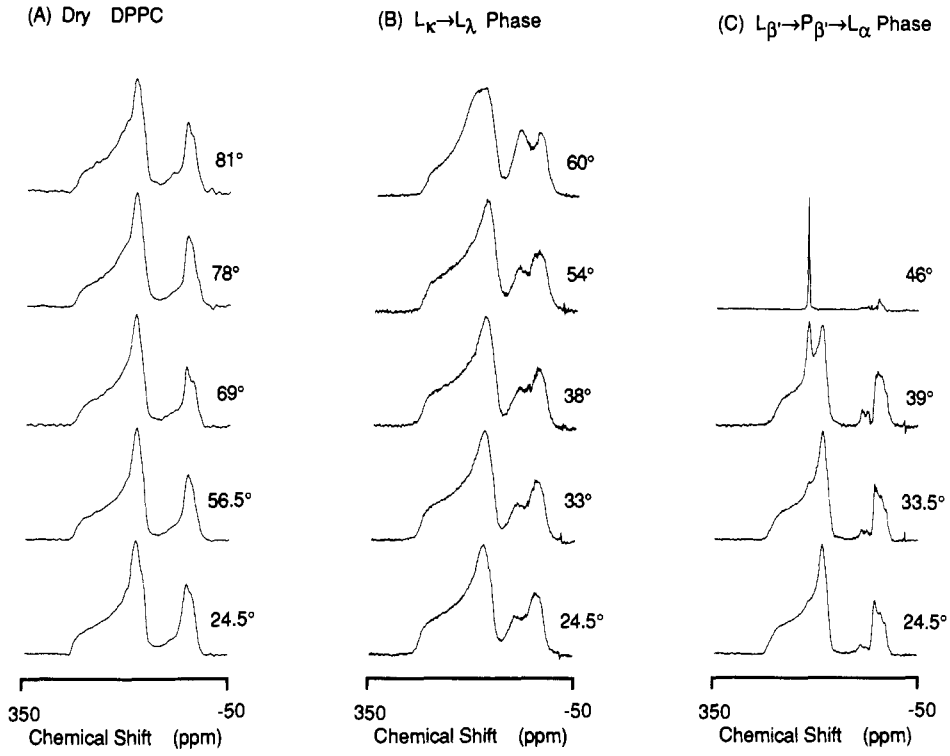

FIGURE 4: Experimental 100.000-MHz ^{13}C NMR spectra of 2[1-^{13}C]DPPC obtained as a function of temperature. (A) Dry 2[1-^{13}C]DPPC; T_m = 77 °C. Acquired with cross-polarization and a subsequent refocusing (180°) pulse. (B) 1.98:1 TRE/2[1-^{13}C]DPPC; $L_\kappa \rightarrow L_\lambda$ transition at 54 °C. (C) Hydrated 2[1-^{13}C]DPPC; $L_{\beta'} \rightarrow P_{\beta'}$ transition at 34.5 °C, $P_{\beta'} \rightarrow L_\alpha$ transition at 42.5 °C. Acquired with a Hahn echo.

reflecting additional librational motion of the choline headgroup.

^2H NMR spectra of hydrated N(C^2H_3)$_3$-DPPC in the $L_{\beta'}$, $P_{\beta'}$, and L_α phases are shown in Figure 3C. The line widths for all spectra are very narrow, and the line shapes contain a small splitting but do not resemble a Pake doublet. There is no change in the line width (FWHM) of 2.9 kHz as the temperature is increased from 24.5 °C ($L_{\beta'}$ phase) to 37 °C ($P_{\beta'}$ phase) and a very slight narrowing of the line width to 1.56 kHz above the main phase transition to the L_α phase at 43 °C. The splitting also decreases from 1.54 kHz in the $L_{\beta'}$ phase to 0.86 kHz in the L_α phase. These spectra reflect extensive motional averaging from all the different rotations, trans-gauche isomerizations, and librational motions available in the headgroup region of hydrated lipids.

^2H NMR spectra from TRE-stabilized N(C^2H_3)$_3$-DPPC can be contrasted with those of dry and hydrated DPPC. The temperature dependence of a 2.14:1 TRE/N(C^2H_3)$_3$-DPPC mixture is shown in Figure 3B. In the L_κ phase at 29.5 °C, the spectrum is 20.3 kHz wide at the base and has a line width (FWHM) of 12.0 kHz. The center of the spectrum exhibits a slight depression. As the temperature is increased, the central depression disappears and grows increasingly rounded. At 48 °C which, is 1 °C below the phase transition temperature, the line shape resembles the room temperature line shape of dry N(C^2H_3)$_3$-DPPC. In the L_λ phase, the line width narrows to 9.46 kHz. From a comparison of the line shapes, it would appear that the rates of reorientation are slightly slower in the TRE/DPPC mixture than in the dry DPPC case. Since the spectrum does not develop into a Pake doublet above the phase transition, we speculate that TRE must be in fairly close contact with the methyl groups and is hindering free rotation of the trimethylamine moiety.

No attempt was made to simulate the line shapes in these samples. The range of motions available are extensive, and any simulation would have to account for internal rotation of the methyl group, reorientation of the methyl groups around the nitrogen, and trans-gauche isomerization of the methylene groups adjacent to the choline moiety as well as librational motions of the whole headgroup (Skarjune & Oldfield, 1979).

Molecular Dynamics of the Interfacial Region. Temperature-dependent NMR spectra of 2[1-^{13}C]DPPC are shown in Figure 4. Again, a direct comparison between dry, hydrated, and TRE-stabilized DPPC bilayers can be made. In Figure 4A, we show the temperature dependence of a dry 2[1-^{13}C]DPPC sample with a phase transition of 77 °C. The spectra show rigid lattice powder patterns for all temperatures both above and below the phase transition. At 24.5 °C, the slightly asymmetric powder pattern exhibits a total width, $\Delta\sigma = \sigma_{11} - \sigma_{33}$, of 144.6 ppm with the principal values σ_{11} = 263.4 ppm, σ_{22} = 140.1 ppm, and σ_{33} = 118.8 ppm. As the sample is heated to above the phase transition, there is a slight, steady decrease in width to 136.1 ppm while retaining the slight asymmetry in the chemical shift tensor. This is consistent with previously published results (Wittebort et al., 1981, 1982).

In contrast to dry DPPC, the hydrated 2[1-^{13}C]DPPC spectra in Figure 4C show pronounced differences as the phase changes from $L_{\beta'}$ to $P_{\beta'}$ to L_α. In the gel-phase $L_{\beta'}$ at 24.5 °C, the width of the axially symmetric powder pattern, $\Delta\sigma = \sigma_\parallel - \sigma_\perp$ is 112.9 ppm with $\sigma_\parallel$ = 247.6 ppm and $\sigma_\perp$ = 134.7 ppm. As the temperature is raised to 39 °C in the $P_{\beta'}$ phase, an isotropic component is apparent. As the sample passes into the L_α phase (T_m = 42.5 °C), the spectrum collapses totally to an isotropic line with a width of 2.44 ppm. This isotropic component is due to a conformational change which occurs at the phase transition and which results in the unique axis of the *sn*-2-carbonyl chemical shift tensor being at the magic angle with respect to the diffusion axis (Wittebort et al., 1981).

Spectra of the TRE-stabilized bilayer are shown in Figure 4B. These spectra from a 1.98:1 TRE/2[1-^{13}C]DPPC sample resemble dry DPPC more than the hydrated DPPC case. In the L_κ phase (below the T_m of 54 °C), the powder pattern has a $\Delta\sigma$ of 148.3 ppm and a very slight asymmetry as manifested by the principal values of σ_{11} = 260.4 ppm, σ_{22} = 138.3 ppm,

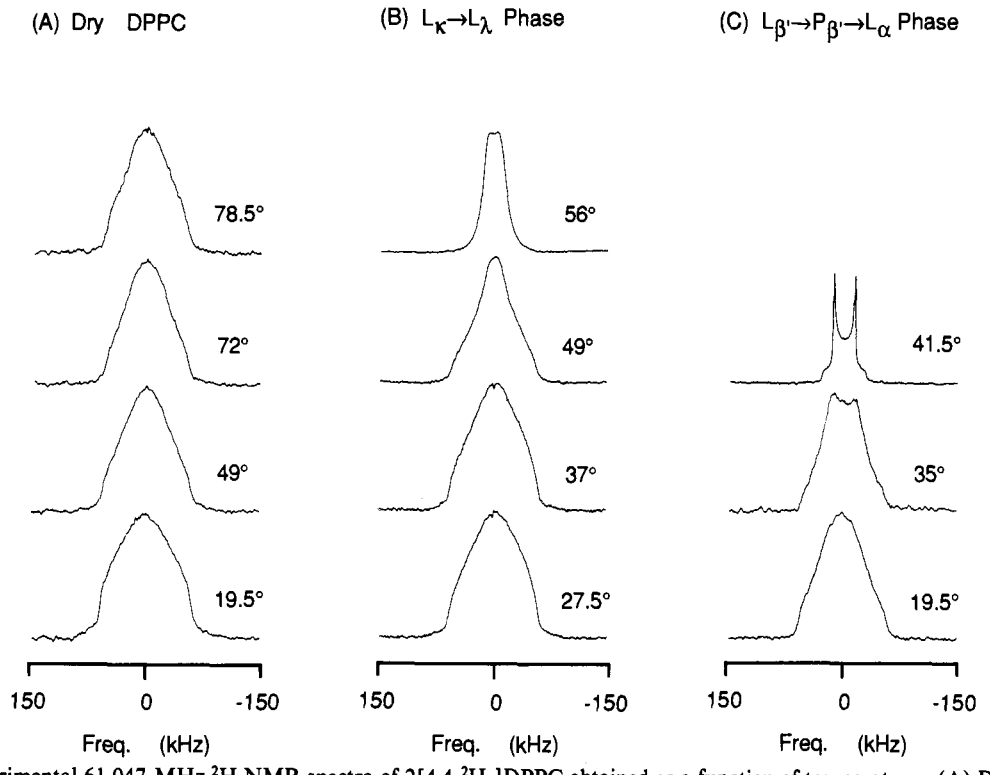

FIGURE 5: Experimental 61.047-MHz ^2H NMR spectra of 2[4,4-$^2H_2$]DPPC obtained as a function of temperature. (A) Dry 2[4,4-$^2H_2$]DPPC; T_m = 75 °C. (B) 1.93:1 TRE/2[4,4-$^2H_2$]DPPC; $L_\kappa \rightarrow L_\lambda$ transition at 49 °C. (C) Hydrated 2[4,4-$^2H_2$]DPPC; $L_{\beta'} \rightarrow P_{\beta'}$ transition at 34.5 °C, $P_{\beta'} \rightarrow L_\alpha$ transition at 41 °C.

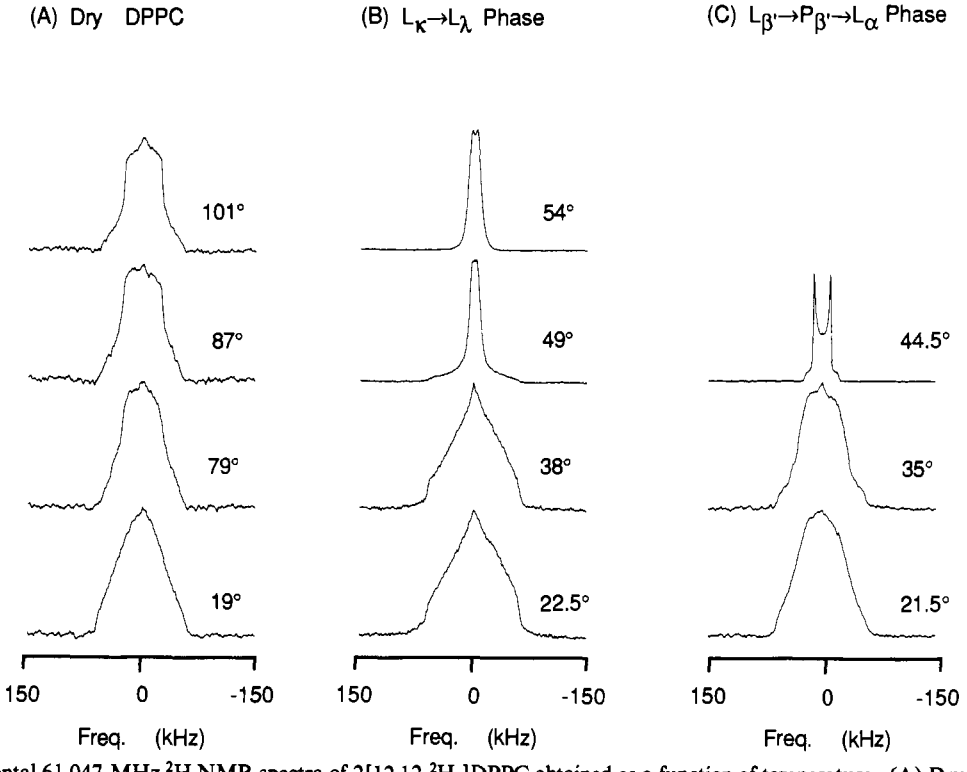

FIGURE 6: Experimental 61.047-MHz ^2H NMR spectra of 2[12,12-$^2H_2$]DPPC obtained as a function of temperature. (A) Dry 2[12,12-$^2H_2$]DPPC; T_m = 95 °C. (B) 2.04:1 TRE/2[12,12-$^2H_2$]DPPC; $L_\kappa \rightarrow L_\lambda$ transition at 49 °C. (C) Hydrated 2[12,12-$^2H_2$]DPPC; $L_{\beta'} \rightarrow P_{\beta'}$ transition at 35 °C, $P_{\beta'} \rightarrow L_\alpha$ transition at 41.5 °C.

and σ_{33} = 112.1 ppm. With increasing temperature, the width of the powder pattern decreases to 142.2 ppm. On passing through the phase transition to the L_λ phase, there is a slight broadening at the edges of the powder pattern, especially at σ_{22} and σ_{33}, but the isotropic component observed in hydrated DPPC is entirely absent. It is clear from these results that at the interfacial region, there is no conformational change and an absence of axial diffusion, since this would average the *sn*-2-carbonyl chemical shift tensor in a very distinctive manner.

Molecular Dynamics of the Hydrocarbon Chain. The ^2H NMR spectra of 2[4,4-$^2H_2$]DPPC and 2[12,12-$^2H_2$]DPPC in dry, hydrated, and TRE-stabilized states are shown in Figures 5 and 6, respectively. These experiments probe the molecular dynamics of different regions of the bilayer interior.

2[4,4-$^2H_2$]DPPC. The temperature dependence of dry 2-

[4,4-$^2H_2$]DPPC is shown in Figure 5A. The spectra are broad and featureless, ranging from a line width (FWHM) of 104.5 kHz at 19.5 °C to 78.1 kHz at 78.5 °C. The base of the spectra was $\simeq$110 kHz at all temperatures. Increasing temperature causes slight narrowing at the center of the spectrum but does not radically change the line shape even above the T_m of 75 °C. These line shapes result from gauche bond formation in the hydrocarbon chain and can be simulated by a two-site hopping model (Wittebort et al., 1987). We did not attempt a full analysis of these line shapes but include this set of spectra as a comparison to the TRE-stabilized system. In the case of dry DPPC, it is known that T_m reflects chain melting, but clearly, positions near the interfacial regions are affected less than positions further down the chain. The C_4-position shows even less motional change than the C_7-position previously studied (Lee et al., 1986).

In Figure 5C, the ^2H spectra of hydrated 2[4,4-$^2H_2$]DPPC are shown at temperatures corresponding to the three different phases, $L_{\beta'}$, $P_{\beta'}$, and L_α. These spectra have been extensively studied and are repeated here solely for comparison with the TRE-stabilized case (Blume et al., 1982; Meier et al., 1986). In the $L_{\beta'}$ phase at 19.5 °C, the spectrum has a width of 116.8 kHz, whereas in the $P_{\beta'}$ phase at 35 °C, shoulders with a line width of 111.0 kHz appear and the center part of the spectrum narrows. Above the main transition of 41 °C, the spectrum transforms to a Pake doublet with $\Delta\nu_{Q\perp}$ = 28.4 kHz. This L_α-phase spectrum reflects fast-limit axial diffusion and extensive trans-gauche isomerization.

The temperature dependence for a 1.93:1 TRE/DPPC mixture, shown in Figure 5B, is of greatest interest. In the L_κ phase, the spectra have a rounded shape similar to the dry DPPC spectra with a line width of 111.3 kHz at 27.5 °C which narrows by <10% as the temperature is increased. These line shapes and widths indicate averaging by two-site motion. In contrast, above the phase transition temperature of 49 °C, the spectrum of the L_λ phase narrows by a factor of $\sim$4 to a width of 31.4 kHz. This line shape is rather featureless with a slightly wider line width than $\Delta\nu_{Q\perp}$ of hydrated DPPC and a poorly resolved splitting of 9.4 kHz in the center of the spectrum. Clearly, the molecular dynamics of the lipid hydrocarbon chains of a TRE-stabilized bilayer are different from that of either the dry or the hydrated bilayer.

2[12,12-$^2H_2$]DPPC. A comparison of 2[12,12-$^2H_2$]DPPC in the dry, hydrated, and TRE-stabilized states is shown in Figure 6. These spectra are very similar to those of 2[4,4-$^2H_2$]DPPC. In the dry 2[12,12-$^2H_2$]DPPC case shown in Figure 6A, the room temperature spectrum at 19 °C has a width of 118.0 kHz. As the temperature neared the transition temperature of 95 °C (this sample was particularly dry), the edges of the spectrum narrowed, and a shoulder similar to that in the $P_{\beta'}$ spectrum of hydrated DPPC developed. The width of the shoulder was 99.1 kHz as compared to the FWHM of 55.7 kHz. Above the phase transition, the line shape develops perpendicular edges and narrows to a line width of 46.4 kHz. The edges of the spectrum begin to resemble a Pake doublet, but the intensity in the center of the spectrum is too large. This indicates that the C_{12}-position of the DPPC hydrocarbon chain is approaching but does not reach fast-limit motion. Thus, for dry lipids, chain melting occurs more readily for positions deep in the hydrophobic core of the bilayer.

The temperature-dependent spectra for hydrated 2[12,12-$^2H_2$]DPPC in the three phases, $L_{\beta'}$, $P_{\beta'}$, and L_α, are shown in Figure 6C. These spectra exhibit line shapes and widths typical of a hydrated lipid. The $L_{\beta'}$ spectrum at 21.5 °C is rounded with a width of 120.5 kHz while in the $P_{\beta'}$ phase at 35 °C, a distinct shoulder appears. The spectrum collapses to a Pake doublet above the main phase transition of 41.5 °C. In the L_α phase, the splitting $\Delta\nu_{Q\perp}$ is 21.5 kHz.

Table I: Comparison of ^2H NMR Spectral Line Widths for the L_α and L_λ Phases

	L_α phase		L_λ phase	
chain position	$\Delta\nu_{Q\perp}$ (kHz)	exptl splitting (kHz)	exptl FWHM (kHz)	simulated FWHM (kHz)
C_4	28.4 (41.5 °C)	9.4 (56 °C)	31.4 (56 °C)	32.5
C_7	28.3 (47 °C)	7.7 (48 °C)	29.3 (48 °C)	29.9
C_{12}	21.5 (44.5 °C)	6.2 (54 °C)	17.5 (54 °C)	21.3

In Figure 6B is the temperature dependence of a 2.04:1 TRE/2[12,12-$^2H_2$]DPPC mixture. The L_κ-phase spectra are broad, "triangular", and not rounded like the other (C_4 and C_7) chain positions. As the temperature is increased, the line width narrows slightly, and the line shape remains "triangular". Above the phase transition temperature of 49 °C in the L_λ phase, there is a spectral narrowing factor of $\sim$6 to a line width of 17.5 kHz. A small splitting of 6.4 kHz is also apparent.

A comparison of the L_λ-phase spectral line widths and the $\Delta\nu_{Q\perp}$'s of the L_α phase is presented in Table I. To date, three hydrocarbon chain positions, 4, 7, and 12, have been studied. These positions were chosen to investigate different parts of the hydrophobic core of the bilayer. In the L_α phase, the Pake doublet splitting, $\Delta\nu_{Q\perp}$, decreases as the chain position is increased, reflecting increased motion toward the end of the chain (Seelig & Seelig, 1974). A similar trend is observed for the TRE-stabilized bilayer. The L_λ-phase line shapes were distinct from either dry or hydrated lipid and did not change significantly from one chain position to another, but the line widths decreased as chain position increased. For the C_4-position, the line width was slightly wider than hydrated DPPC. However, a line width of 30.3 kHz was previously published for hydrated 1,2[4,4-$^2H_2$]DPPC (Seelig & Seelig, 1974) so that the difference reported here may be insignificant. The small poorly resolved splitting at the center of the spectra also showed a steady decrease as the chain position increased, from 9.4 kHz at the C_4-position to 6.4 kHz at the C_{12}-position. The splitting is also more pronounced at the end of the chain as compared to positions close to the headgroup.

Computer Simulations of L_λ Line Shapes. Before describing the computer model used to fit these unusual L_α-phase ^2H NMR spectra, we include a short summary of how dynamic processes affect the ^2H NMR powder line shape, especially in the intermediate exchange regime ($\omega_Q\tau_c \sim 1$) (Rice et al., 1987; Beshah et al., 1987; Griffin et al., 1988). For motional averaging in this intermediate regime, T_2 becomes anisotropic and $\leq\tau$ (the pulse spacing in the echo sequence) for many orientations in the powder sample. Here, much of the signal decays and is not refocused by the second pulse. This leads to dramatic spectral intensity losses as well as line-shape changes. In addition, the spectra will also exhibit a τ dependence, both in spectral intensity and in line shape, as the pulse spacing is lengthened. Any dynamic model used in simulating these spectra must therefore faithfully reproduce not only the intensity losses but also the τ-dependent line shapes.

For systems where the motional averaging tends to the fast limit, an additional set of parameters can be used to constrain the simulation. T_1 is also anisotropic across the powder pattern, and simulated spectra should reproduce both the line shapes and zero-crossing for an inversion recovery experiment.

The model used for the line-shape calculations consists of

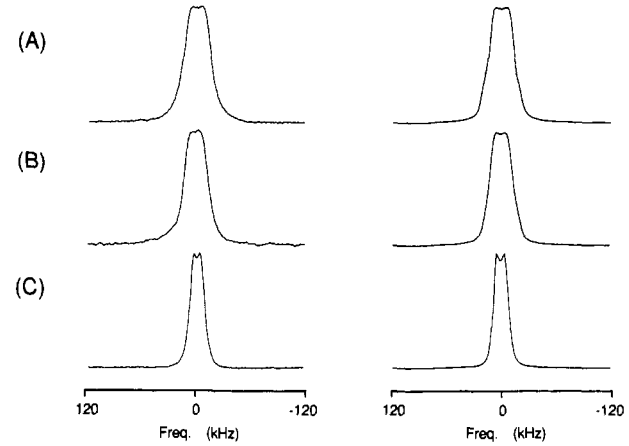

FIGURE 7: Computer simulations of the molecular dynamics of the hydrocarbon chain in the L_λ phase. (Left) Experimental 61.047-MHz ^2H NMR spectra. (Right) Line-shape simulations of the experimental spectra. (A) Parameters for the C_4-position: four-site hops, all angles = 109.5°, P_1:P_2:P_3:P_4 = 0.31:0.30:0.27:0.12 (±0.01), $k_{12} = k_{13} = k_{14}$ = 1.6 (±0.2) × 10^7 s^{-1}. (B) Parameters for the C_7-position: four-site hops, all angles = 109.5°, P_1:P_2:P_3:P_4 = 0.30:0.30:0.26:0.14 (±0.01), $k_{12} = k_{13} = k_{14}$ = 2.0 (±0.2) × 10^7 s^{-1}. (C) Parameters for the C_{12}-position: $\angle D_1$–C–D_2 = 109.5°/$\angle D_3$–C–D_4 = 100°, P_1:P_2:P_3:P_4 = 0.27:0.27:0.23:0.23 (±0.01), $k_{12} = k_{13} = k_{14}$ = 1.0 (±0.2) × 10^8 s^{-1}.

a deuteron hopping among defined sites with a certain probability for the occupation of a site and a particular jump rate between sites (Wittebort et al., 1987). Since axial diffusion of the whole lipid molecule is quenched in the L_λ phase, the only motion available is trans-gauche isomerization of the polymethylene chain among tetrahedral sites. The results of the computer simulations of the L_λ line shapes together with experimental spectra from the C_4-, C_7-, and C_{12}-labeled lipid are shown in Figure 7.

The simulation parameters for each spectrum are listed in the figure captions, and a comparison of the experimental and simulated line widths is shown in Table I. Inspection of Figures 7 and 8 reveals that the simulations fit remarkably well. In order to reduce the spectral widths to ~20–30 kHz, it was necessary to employ a four-site jump model with approximately equal populations. A common feature for all chain positions is the small splittings in the center of the spectrum. To adequately reproduce these features, it was necessary to introduce some sort of asymmetry into the simulation either as an asymmetric skewing of the site populations or by changing the geometry between the third and fourth sites. For the C_4- and C_7-positions, tetrahedral angles between all sites and skewed populations were employed, but for the 12-position, the angle, $\angle D_3$–C–D_4, had to be changed to 100°. The change was necessitated by the extremely narrow line width of the spectrum coupled with the small splitting in the center. The significance of such a change will be discussed below.

Due to the large number of variables involved in the simulations, it is possible that different sets of parameters will yield similar line shapes. To ensure that the simulation parameters are correct, it is necessary to examine the τ dependence of both the line shape and the spectral intensities. The experimental and simulated spectral intensities for L_α spectra from the C_4- and C_7-positions are shown in Figure 8. The results agree remarkably well. The experimental line shape does not change as τ is varied. This feature is also reproduced by the computer simulation (results not shown).

As a final check, T_1 measurements were made on a 2:1 TRE/2[4,4-$^2H_2$]DPPC sample (results not shown). The experimental T_1 value of 25.0 ms corresponded closely to the

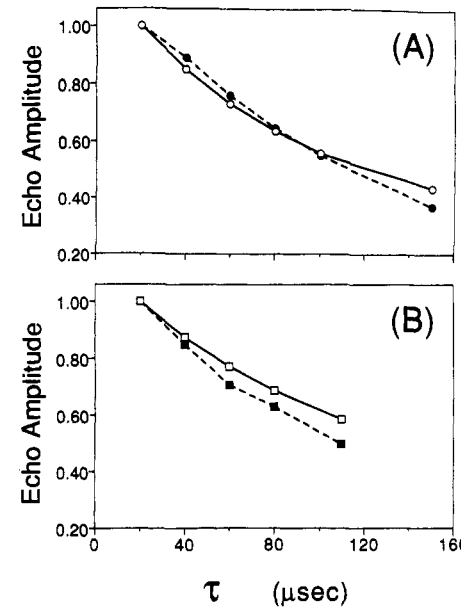

FIGURE 8: Comparison between computer simulation and experimentally determined spectral intensities as a function of τ, the pulse spacing in the quadrupole echo sequence. The amplitudes are normalized to 20 μs, the shortest pulse spacing employed. (A) τ-dependent spectral intensities for C_4. (●) Experimental intensities; (○) computer-simulated intensities. (B) τ-dependent spectral intensities for C_7. (■) Experimental intensities; (□) computer-simulated intensities.

simulated value of 22.9 ms using the simulation parameters reported above. Thus, within the context of the motional model employed for the calculations, the simulations appear to be unique.

Discussion

The analysis of the X-ray diffraction patterns of the TRE/DPPC mixtures suggests a lipid bilayer embedded in a disaccharide matrix. It is not possible to determine quantitatively the stoichiometry of the complex, but, due to the excess TRE in the sample, clearly we are observing the full effects of the sugar on the bilayer. However, without a knowledge of the chain tilt angle, it is impossible to estimate the thickness of the TRE matrix.

The X-ray results also reflect the metastability of the $L_\kappa \rightarrow L_\lambda$ transition. On recooling, the diffraction pattern is similar to but not identical with that obtained before heating. The low-angle reflections revert to their original intensity distribution, but the 4.12-Å reflection is somewhat sharper compared to the diffraction pattern obtained before heating. The bilayer periodicity is also reduced from the preheated value which perhaps reflects either (a) the increased disorder in the metastable state on recooling or (b) a rearrangement of the interbilayer sugar lattice.

From the X-ray and NMR studies probing the structure and dynamics of the different regions of the bilayer, a more complete picture of the phases in a TRE-stabilized dry membrane has emerged. Previously, we have shown that the phosphate moiety of the lipid was completely immobilized by the sugar. In addition, we now have evidence that even the dynamics of the methyl groups in the choline moiety are affected by the close proximity of TRE. In particular, the methyl groups in the TRE/DPPC mixture are still undergoing some sort of nine-site motion, but on a time scale slightly slower than that of dry DPPC. As indicated by the ^{13}C NMR studies at the *sn*-2-carbonyl position, the interfacial region of the phospholipid is also affected by the presence of TRE, resulting in the observation of rigid lattice spectra.

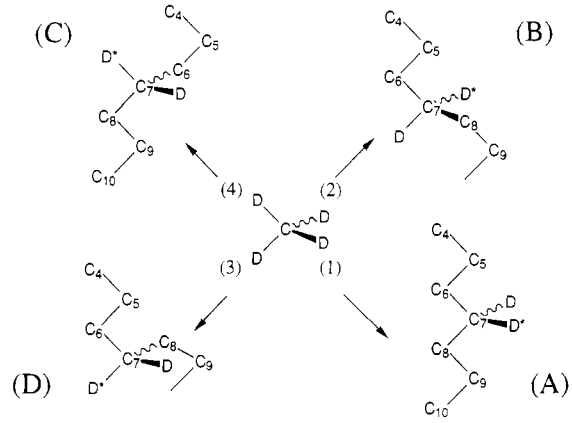

FIGURE 9: Illustration of how the four C–D orientations in a diamond lattice can be populated by trans-gauche isomerization. The C_7-position is (arbitrarily) assumed to be the central carbon. The two C–D bonds of a methylene group are magnetically equivalent. (Center) The four C–D tensor orientations are located along tetrahedral angles. (A) An all-trans chain (tttttt) with the D* atom in the first site. (B) Population of the second site by a ttg^+tg^-t kink. (C) Population of the third site by a ttg^-tg^+t kink. (D) Population of the fourth site by a tg^-tg^+tt kink.

The ^2H NMR line-shape studies of the hydrocarbon chain dynamics are consistent with increasing motion down the chain. The line shapes associated with the L_λ phase are unique to the sugar-stabilized bilayer, and apparently arise from fast-limit motions due to trans-gauche isomerization in the absence of axial diffusion of the lipid molecule. The effect of TRE on the bilayer structure is best appreciated when one compares the results with data from dry DPPC above its phase transition. Clearly, dry DPPC has a much more closely packed lattice than do TRE/DPPC mixtures. Without an expanded area between each lipid molecule, gauche bond formation is inhibited, and the spectra would not exhibit the extreme narrowing observed in these studies.

The L_λ-phase line shapes can be successfully simulated by a model that assumes only trans-gauche isomerization. This model (Wittebort et al., 1987) assumes that the deuteron of a C–D bond in a hydrocarbon chain is hopping among defined sites in a diamond lattice. Although both hydrogen atoms of the methylene group are deuterated, only one of the C–D bond needs to be considered because of the two bonds are magnetically equivalent. The probability of occupation of a site other than the first site is associated with the formation of a gauche bond. However, due to space considerations in the lipid lattice, an isolated gauche bond is rare, with a *gtg'* kink being the more common manifestation of chain disorder. As an example, we show in Figure 9 the manner in which all four of the diamond lattice sites for the C_7-position can be populated by the appropriate isomerization of the bonds C_6–C_7 or C_8–C_9. An all-trans chain as shown in Figure 9A would be manifest as a large occupational probability (P) of one of the four sites. Simple *gtg'* kink formation would result in the population of a second site on the lattice. Instances of higher chain disorder would result in *gtg'* kinks traveling up and down the chain in a "crankshaft motion" and would result in occupation of the third and fourth sites in the lattice as shown in Figure 9B–D.

Note that in most NMR experiments, labeling of the hydrocarbon chain in one position results in an experiment that probes motions only in that specific region of the molecule. Multiple kinks propagating above and below the labeled position in a perfect lattice would be indistinguishable from a single kink. Moreover, phospholipid molecules do not exhibit perfect chain packing even in a single crystal (Pearson & Pascher, 1979). There is a slight twist (12° in DMPC) as one moves down the chain so that the methylene groups do not stack perfectly on top of one another. Coupled with the multiple propagating kinks in the chain, this leads to a disordered lattice especially toward the end of the chain. The requirement for a diamond lattice was relaxed in the simulations for the C_{12}-position in an effort to account for the disorder. Specifically, the D_3–C–D_4 angle was changed from 109.5° to 100°. For the other chain positions, this correction was unnecessary, and tetrahedral angles were used.

From the NMR evidence, we can draw certain conclusions about the structure of the L_κ and L_λ phases in TRE-stabilized bilayers. First, the sugar is in close proximity with the hydrophilic region of the lipid from the headgroup to the interfacial regions as is evident from the hindered molecular dynamics of all the functional groups studied. The eight hydroxyl groups on each TRE molecule are all available for hydrogen bonding to the phosphate and carbonyl groups, although we have no indication whether each sugar molecule complexes with one lipid or more lipid molecules. The hindered motion of the choline moiety is most likely due to a steric effect of the TRE since hydrogen bonding to a quaternary ammonium ion is unlikely. A second observation is that the sugar must occupy some space *between* lipid molecules. This is in contrast to the model proposed by Chandrasekhar and Gaber (1988) where the sugar fits *on top of* the lipid headgroups in a close-packed crystalline lattice of lipid molecules. If the sugar merely occupied an interstitial space in the lipid lattice, then the hydrocarbon chain NMR spectra of a TRE/DPPC mixture would resemble that of dry DPPC and would not exhibit the extensive motions as indicated by the computer simulations on our NMR results.

CONCLUSIONS

In this paper, we have presented results from X-ray diffraction and solid-state NMR studies which characterize the L_κ and L_λ phases in TRE-stabilized bilayers. The L_κ and L_λ phases differ from the phases in any dry or hydrated lipids studied to date. The X-ray diffraction results of the L_κ phase show some of the reflections usually attributable to gel-phase lipid. Similarly, reflections indicative of the chain-melted state also occur in diffraction patterns of the L_λ phase. The NMR studies of TRE-stabilized bilayers showed significant differences from hydrated bilayers while revealing a number of interesting similarities. The interaction of TRE on the hydrophilic part of the phospholipid entirely inhibited axial diffusion of the lipid molecules in the bilayer. Headgroup and interfacial regions showed either an absence of motional averaging (phosphate and the *sn*-2-carbonyl moieties) or a hindered motional averaging (choline moiety). In contrast, the hydrocarbon chains exhibited extensive trans-gauche isomerization, especially in the L_λ phase, which was successfully analyzed by computer simulation of the ^2H NMR line shapes. This chain disorder is possible if one postulates a bilayer structure where the TRE is intercalated between lipid molecules, thus acting as a spacer to expand the bilayer. The resultant TRE-stabilized system mimics the extensive chain disorder in the L_α phase of hydrated lipid. Thus, the TRE-stabilized bilayer may be playing an important role in maintaining membrane structure and cell viability in the dehydrated state.

ACKNOWLEDGMENTS

We thank Dr. K. Beshah and J. Speyer for stimulating discussions during the course of this work.

Registry No. TRE, 99-20-7; DPPC, 63-89-8; 2[4,4-$^2H_2$]DPPC, 120205-73-4; 2[12,12-$^2H_2$]DPPC, 120205-74-5; 2[1-^{13}C]DPPC, 65277-92-1; N(C^2H_3)$_3$-DPPC, 77165-56-1; DPPE, 923-61-5; 2[4,4-

$^2H_2$]palmitic acid, 30719-28-9; 2[12,12-$^2H_2$]palmitic acid, 120205-75-6.

REFERENCES

Arnett, E. A., Harvey, N., Johnson, E. A., Johnston, D. S., & Chapman, D. (1986) *Biochemistry 25*, 5239–5242.

Beshah, K., Olejniczak, E. T., & Griffin, R. G. (1987) *J. Chem. Phys. 86*, 4730–4736.

Bloom, M., Davis, J. H., & Valic, M. I. (1980) *Can. J. Phys. 58*, 1510–1517.

Blume, A., Wittebort, R. J., Das Gupta, S. K., & Griffin, R. G. (1982) *Biochemistry 21*, 6243–6253.

Chandrasekhar, I., & Gaber, B. (1988) *J. Biomol. Struct. Dyn. 5*, 1163–1171.

Chapman, D., Williams, R. M., & Ladbrooke, B. D. (1967) *Chem. Phys. Lipids 1*, 445–475.

Clegg, J. S. (1965) *Comp. Biochem. Physiol. 14*, 135–143.

Clegg, J. S., Seitz, P., Seitz, W., & Hazlewood, C. F. (1982) *Cryobiology 19*, 306–316.

Crowe, J. H., & Clegg, J. S. (1973) *Anhydrobiosis*, Dowden, Hutchison and Ross, Inc., Stroudsburg, PA.

Crowe, J. H., & Clegg, J. S. (1979) *Dry Biological Systems*, Academic Press, New York.

Crowe, J. H., & Crowe, L. M. (1984) in *Biological Membranes* (Chapman, D., Ed.) Vol. 5, pp 58–103, Academic Press, New York.

Crowe, J. H., Crowe, L. M., & Jackson, S. A. (1983) *Arch. Biochem. Biophys. 220*, 477–484.

Crowe, J. H., Crowe, L. M., & Chapman, D. (1984) *Science 223*, 701–703.

Crowe, L. M., Mouradian, R., Crowe, J. H., Jackson, S. A., & Womersley, C. (1984) *Biochim. Biophys. Acta 769*, 141–150.

Crowe, L. M., Womersley, C., Crowe, J. H., Reid, D., Appel, L., & Rudolph, A. (1986) *Biochim. Biophys. Acta 861*, 131–140.

Das Gupta, S. K., Rice, D. M., & Griffin, R. G. (1982) *J. Lipid Res. 23*, 197–200.

Davis, J. H., Jeffrey, K. R., Bloom, M., Valic, M. I., & Higgs, T. P. (1976) *Chem. Phys. Lett. 42*, 390–394.

Griffin, R. G. (1981) *Methods Enzymol. 72*, 108–174.

Griffin, R. G., Beshah, K., Ebelhaüser, R., Huang, T. H., Olejniczak, E. T., Rice, D. M., Siminovitch, D. J., & Wittebort, R. J. (1988) in *The Time Domain in Surface and Structural Dynamics* (Long, G. J., & Grandjean, F., Eds.) pp 81–105, Reidel Publishing Co., Dordrecht, Holland.

Gupta, C. M., Radhakrishnan, R., & Khorana, H. G. (1977) *Proc. Natl. Acad. Sci. U.S.A. 74*, 4315–4319.

Janiak, M. J., Small, D. M., & Shipley, G. G. (1979) *J. Biol. Chem. 254*, 6068–6078.

Johnston, D. S., Coppard, E., Parera, G. V., & Chapman, D. (1984) *Biochemistry 23*, 6912–6919.

Lee, C. W. B., Waugh, J. S., & Griffin, R. G. (1986) *Biochemistry 25*, 3737–3742.

Leopold, A. C. (1986) *Membranes, Metabolism and Dry Organisms*, Cornell University Press, Ithaca, NY.

Madin, K. C., Crowe, J. H., & Loomis, S. H. (1979) in *Dry Biological Systems* (Crowe, J. H., & Clegg, J. S., Eds.) pp 155–174, Academic Press, New York.

Meier, P., Ohmes, E., & Kothe, G. (1986) *J. Chem. Phys. 85*, 3598–3614.

Patel, K. M., Morrisett, J. D., & Sparrow, J. T. (1979) *Lipids 14*, 596–590.

Pearson, R. H., & Pascher, I. (1979) *Nature 281*, 499–501.

Pines, A., Gibby, M. G., & Waugh, J. S. (1973) *J. Chem. Phys. 59*, 569–590.

Rice, D. M., Meinwald, Y. C., Scheraga, H. A., & Griffin, R. G. (1987) *J. Am. Chem. Soc. 109*, 1636–1640.

Seelig, A., & Seelig, J. (1974) *Biochemistry 13*, 4839–4845.

Skarjune, R., & Oldfield, E. (1979) *Biochemistry 18*, 5903–5909.

Tardieu, A., Luzzati, V., & Reman, F. C. (1973) *J. Mol. Biol. 75*, 711–733.

Vega, A. J., & Luz, Z. (1987) *J. Chem. Phys. 86*, 1803–1813.

Wittebort, R. J., Schmidt, C. F., & Griffin, R. G. (1981) *Biochemistry 20*, 4223–4228.

Wittebort, R. J., Blume, A., Huang, T.-H., Das Gupta, S. K., & Griffin, R. G. (1982) *Biochemistry 21*, 3487–3502.

Wittebort, R. J., Olejniczak, E. T., & Griffin, R. G. (1987) *J. Chem. Phys. 86*, 5411–5420.